OPEN BIOLOGY

royalsocietypublishing.org/journal/rsob

Research

Cite this article: Haniffa S, Narain P, Hughes MA, Petković A, Šušić M, Mlambo V, Chaudhury D. 2023 Chronic social stress blunts core body temperature and molecular rhythms of *Rbm3* and *Cirbp* in mouse lateral habenula. *Open Biol.* **13**: 220380.
https://doi.org/10.1098/rsob.220380

Received: 26 December 2022
Accepted: 29 June 2023

Subject Area:
neuroscience/systems biology

Keywords:
temperature rhythms, chronic stress, mood disorder, thermosensitive gene, suprachiasmatic nucleus, lateral habenula

Author for correspondence:
Dipesh Chaudhury
e-mail: dc151@nyu.edu

†These authors contributed equally to this work.

Electronic supplementary material is available online at https://doi.org/10.6084/m9.figshare.c.6730010.

THE ROYAL SOCIETY PUBLISHING

Chronic social stress blunts core body temperature and molecular rhythms of *Rbm3* and *Cirbp* in mouse lateral habenula

Salma Haniffa[1,†], Priyam Narain[2,†], Michelle Ann Hughes[1], Aleksa Petković[1], Marko Šušić[1], Vongai Mlambo[1] and Dipesh Chaudhury[1]

[1]Department of Biology, Science Division and [2]Centre for Genomics and Systems Biology (CGSB), New York University Abu Dhabi, Abu Dhabi, United Arab Emirates

DC, 0000-0001-8014-6373

Chronic social stress in mice causes behavioural and physiological changes that result in perturbed rhythms of body temperature, activity and sleep-wake cycle. To further understand the link between mood disorders and temperature rhythmicity in mice that are resilient or susceptible to stress, we measured core body temperature (Tcore) before and after exposure to chronic social defeat stress (CSDS). We found that Tcore amplitudes of stress-resilient and susceptible mice are dampened during exposure to CSDS. However, following CSDS, resilient mice recovered temperature amplitude faster than susceptible mice. Furthermore, the interdaily stability (IS) of temperature rhythms was fragmented in stress-exposed mice during CSDS, which recovered to control levels following stress. There were minimal changes in locomotor activity after stress exposure which correlates with regular rhythmic expression of *Prok2* - an output signal of the suprachiasmatic nucleus. We also determined that expression of thermosensitive genes *Rbm3* and *Cirbp* in the lateral habenula (LHb) were blunted 1 day after CSDS. Rhythmic expression of these genes recovered 10 days later. Overall, we show that CSDS blunts Tcore and thermosensitive gene rhythms. Tcore rhythm recovery is faster in stress-resilient mice, but *Rbm3* and *Cirbp* recovery is uniform across the phenotypes.

1. Introduction

Daily cycles of light and temperature are the two primary environmental timing cues used by living systems to entrain their endogenous circadian rhythms to the astronomical day. In mammals, the suprachiasmatic nucleus (SCN), the principal biological clock, drives circadian rhythms of core body temperature (Tcore), which is maintained within a narrow range to allow for optimal physiological functioning [1,2]. These rhythms can be entrained by external cues, predominantly light, but in the absence of these cues they exhibit endogenous free running characteristics. In homeothermic organisms Tcore is measured by internal and peripheral thermoreceptors [3]. The preoptic area of the hypothalamus is the primary integrative site for thermoregulation [4]. The narrow range of Tcore rhythms is maintained by a complex feedback system consisting of heat-loss mechanisms that are activated when Tcore temperature rises, as well as heat-gain mechanisms which are activated when it falls [5–7]. It is hypothesized that daily Tcore rhythms are generated by SCN neurons projecting into hypothalamic regulatory centers and by modulation of thermogenic brown adipose tissue [8]. Tcore is an intrinsic zeitgeber (ZT) since changing the amplitude and frequency of temperature rhythms affects the rhythmic

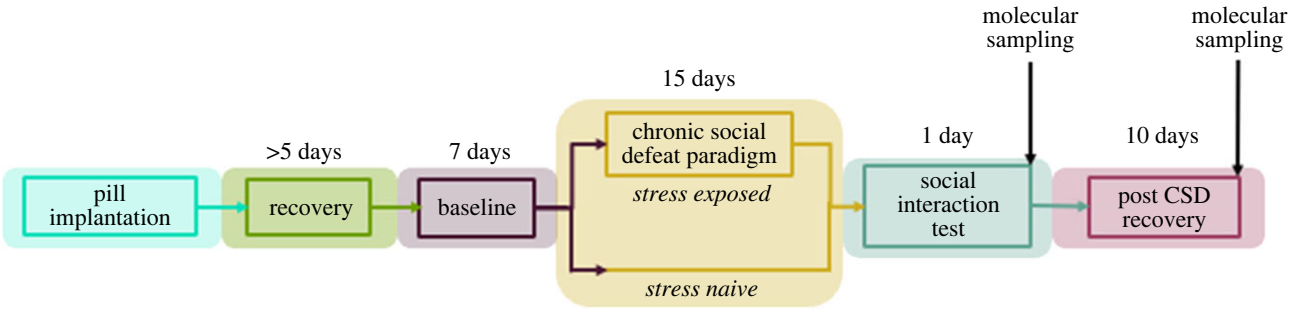

Figure 1. Timeline for investigating the association between stress, diurnal temperature rhythms and changes in expression of thermosensitive genes.

expression of key clock genes: Basic Helix-Loop-Helix ARNT Like 1 (*Bmal1*) and Period 1 (*Per1*) [9]. These changes are likely driven by changes in expression of thermo-sensitive genes, such as RNA-binding Motif Protein 3 (*Rbm3*), Cold-inducible RNA binding protein (*Cirbp*) and Heat Shock Factor 1 (*Hsf1*), which are chaperones that modulate expression of a variety of target genes including the clock genes [7,10–13].

Mood disorders and aberrations in Tcore rhythms are closely related. Patients often exhibit a shift or blunting of diurnal cortisol and Tcore rhythmic activity during depressive episodes [14,15]. The association between circadian rhythms and depression is commonly attributed to molecular and pathophysiological changes in brain circuits that coregulate emotions, locomotor activity, sleep and body temperature [16]. Although clinical studies indicate a relationship between desynchronization of Tcore rhythms and symptom severity, it is unclear whether the relationship is correlational or causal [15]. While the effects of stress on activity, sleep-wake cycle and molecular rhythms have been investigated, mechanisms linking stress and Tcore rhythms are understudied.

Stress-induced thermogenesis of brown adipose tissue that results in emotional hyperthermia is thought to be driven by the lateral habenula (LHb) and ventral tegmental area (VTA) [17,18] - two key brain regions that exhibit elevated pathophysiological firing in stress-susceptible mice [19–22]. Pathophysiological changes in these regions may be responsible for stress-induced changes in temperature rhythms. Furthermore, onset of a variety of mood disorders has been associated with changes in circadian rhythms of molecular processes in the SCN and LHb [20,23]. At the transcriptome level, *Rbm3* and *Cirbp* are expressed in response to lower temperatures while *Hsf1* is expressed in response to heat stress [24]. Patients with mood disorders exhibit a higher expression of *Rbm3* compared to healthy controls [25]. Deletion of *Rbm3* leads to a significant reduction in expression amplitudes of clock genes *Bmal1*, *Clock*, *Per1* and *Cry1* Cryptochrome 1(*Cry1*) [10]. In the cell nucleus, *Cirbp* binds to the 3′-UTR of *Clock* mRNA and promotes its translocation to the cytoplasm, thereby enabling its translation [11–13]. *Hsf1* interacts with clock genes, such as *Bmal1*, in order to maintain synchronization of the cellular clock and clock-controlled adaptive responses to cellular stress [26]. Absence of *Hsf1* activity can lead to impaired hippocampal development and severe behavioural disruptions, such as depression and elevated aggression [27].

To understand the association between Tcore and mood disorders we used the chronic social defeat stress (CSDS) paradigm to investigate the effects of chronic stress on Tcore and expression of *Cirbp*, *Rbm3* and *Hsf1* (figure 1). Prior to stress all mice exhibited similar daily Tcore rhythms. During CSDS both stress-resilient and susceptible mice exhibited blunted Tcore rhythms. During the first 5 days of post-CSDS recovery period, Tcore amplitudes were significantly blunted in susceptible, but not resilient, mice compared to controls. By days 6–10 of post-CSDS recovery, the average Tcore amplitude of susceptible mice returned to control levels (figure 2). Furthermore, stress-exposed mice exhibited fragmented temperature rhythms during CSDS, which was consolidated in the recovery phase. Control mice exhibited daily rhythmic expression of *Rbm3* and *Cirbp* in the LHb where transcript levels were higher in the day than the night – in concordance with decreased core body temperature in the day compared to the night (figure 3). By contrast, rhythmic expression of *Rbm3* and *Cirbp* expression was blunted 1-day post-CSDS in both resilient and susceptible mice which returned to control levels after 10 days of recovery. *Hsf1* did not exhibit diurnal rhythmic expression in the LHb of control mice and was not impacted by stress exposure (electronic supplementary material, figure S5). *Prok2* expression in the SCN was unaffected by stress exposure as all mice exhibited high relative expression in the day and low at night which likely correlates with normal locomotor rhythms in mice exposed to stress (electronic supplementary material, figures S3 and S4). *BMAL1* expression likewise did not differ between the phenotypes (electronic supplementary material, figure S4).).

2. Methods

2.1. Animals

C57BL6/J mice of 5–7 weeks old were purchased from Jackson Laboratory (Bar Harbor, Maine, USA). Single-housed male CD1 retired breeder mice from Charles River laboratory (Wilmington, Maine, USA) were used as resident aggressors for the CSDS paradigm. All experimental mice were maintained within standard housing conditions at a temperature of 21 ± 2°C and humidity of 50 ± 10% with *ad libitum* access to food and water, and enrichment in the form of wood shavings. Mice were kept on a 12 : 12 h light/dark cycle, with light onset at 07.00 (ZT0) and light offset at 19.00 (ZT12). Temperature, locomotor and gene expression experiments were done on the same mouse cohorts.

2.2. Core body temperature recordings

Mice were anesthetized with a ketamine (100 mg kg^{-1}) and xylaxine (10 mg kg^{-1}) mixture. A wireless electronic telemetry

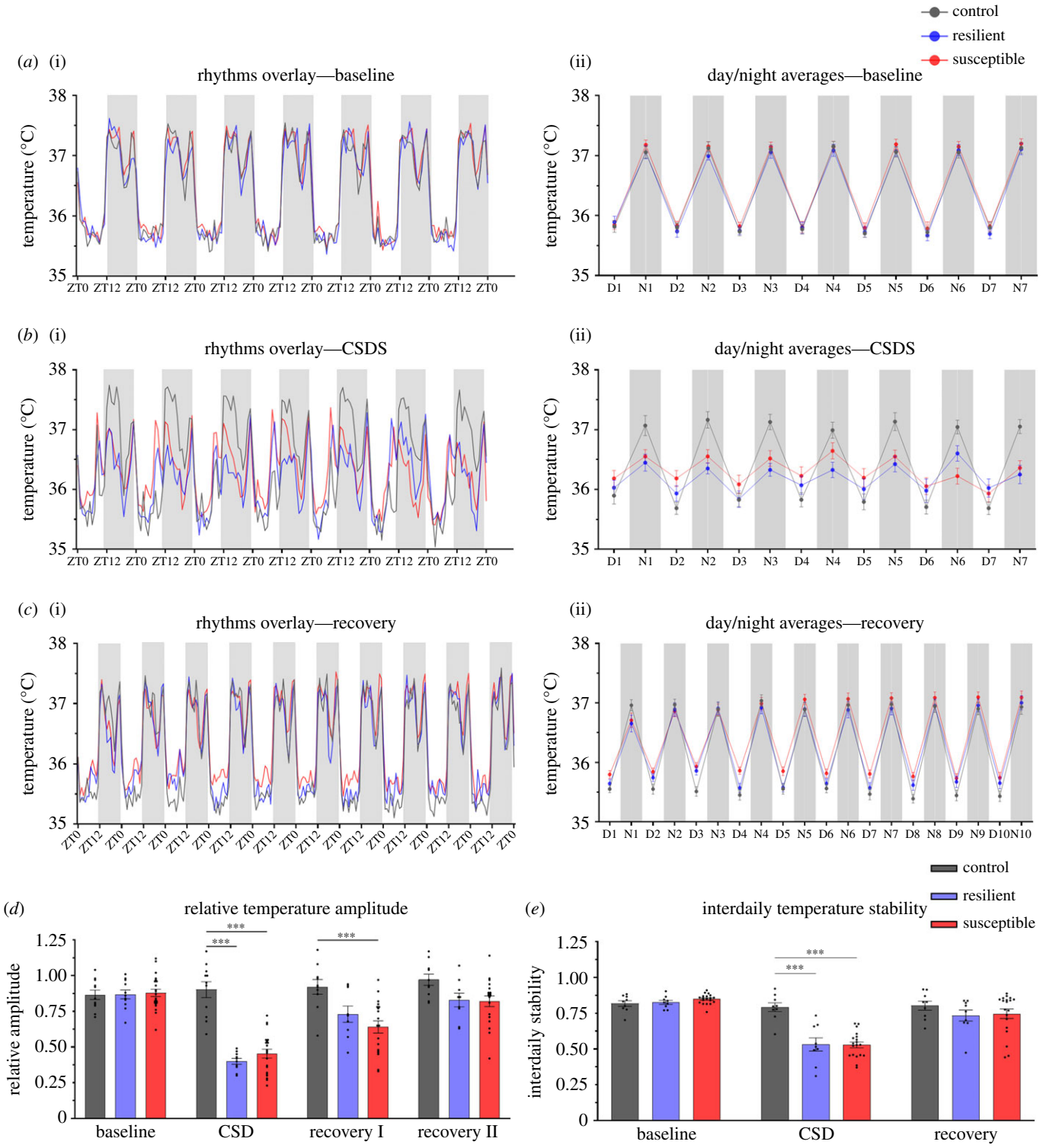

Figure 2. (*Caption overleaf.*)

pill (Anipill; BodyCap, Paris, France) was surgically implanted into the peritoneal cavity of all experimental mice. This surgical implantation was carried out by adopting and modifying previously published protocol [28]. The Anipill system was configured to collect temperature measurements every 15 min. Temperature recordings were set to begin immediately after pill activation and continued to collect and transmit data for the entire duration of the experiment. Open-source online software Biodare2 was used to extract circadian parameters such as amplitude, phase, and period of temperature rhythms [29]. Fast Fourier transform nonlinear least squares (FFT NLLS) was employed to analyze average hourly data. Interdaily stability analysis was conducted in R (v. 4.1.1) following previously published equations [30,31].

2.3. Locomotor activity recording

Locomotor activity during baseline and recovery periods was continuously measured using Actimetrics ClockLab wireless passive infrared (PIR) sensor system (Actimetrics, Chicago, Illinois, USA). The infrared sensor was placed on top of each small hamster cage, which were used to single-house the mice. The data was collected using ClockLab Data

Figure 2. (*Overleaf.*) Average core body temperature rhythms during baseline, CSDS and recovery. Temperature values include recordings from 7 days of baseline, last 7 days of CSDS and 10 days of recovery. (*a*)(i) Control, resilient and susceptible mice show comparable Tcore rhythms prior to CSDS in 12H:12H light/dark conditions. (*b*)(i) CSDS blunts the temperature amplitude of resilient and susceptible mice compared to controls ($n = 11$). (*c*)(i) The Tcore of susceptible mice remains blunted longer than resilient mice during the recovery period. (*a–c*)(ii) Average day and night values (averaging 12 h day and night separately for each phenotype) of Tcore during baseline, CSDS and recovery. Baseline: no significant difference between phenotypes. CSDS: susceptible and resilient mice exhibit significantly lower Tcore most nights compared to controls. Two-way ANOVA revealed significant main effect of phase ($F_{13,462} = 21.90$, $p < 0.001$), phenotype ($F_{2,462} = 11.36$, $p < 0.001$), and interaction between the two factors ($F_{26,462} = 4.738$, $p < 0.001$). In most nights, resilient and susceptible mice exhibited significantly lower average Tcore compared to controls (electronic supplementary material, table S1). Recovery: daytime Tcore of susceptible mice was significantly higher relative to controls for most days following CSDS. Two-way ANOVA shows significant effects of phase ($F_{19,660} = 148.7$, $p < 0.001$) and phenotype ($F_{2,660} = 20.08$, $p < 0.001$). Daytime Tcore averages of susceptible mice during recovery were higher on most days relative to controls (electronic supplementary material, table S2). (*d*) Baseline: there was no difference in baseline Tcore amplitude between the phenotypes. CSDS: Tcore amplitude was significantly blunted in susceptible and resilient mice during CSDS relative to controls (electronic supplementary material, table S2). Recovery: susceptible and resilient mice exhibited significantly blunted amplitude relative to the controls during the first 5 days of recovery. Temperature amplitude recovers to control levels in days 6–10. (*e*) Interdaily stability of the temperature rhythms during baseline, CSDS and recovery were calculated for each phenotype. Two-way ANOVA shows significant effects of phase ($F_{2,64} = 62.3$, $p < 0.001$), phenotype ($F_{2,34} = 6.24$, $p < 0.01$) and interaction ($F_{4,\ 68} = 11.9$, $p < 0.001$). Baseline: there was no difference in Tcore rhythm stability between the phenotypes. CSDS: susceptible (Tukey's HSD, $p < 0.001$, 95% C.I. = [0.17, 0.36]) and resilient mice ($p < 0.001$, 95% C.I. = [0.11, 0.40]) exhibit significantly lower Tcore rhythm stability relative to controls. Recovery: there was no difference in Tcore rhythm stability between the phenotypes. (*a–e*) Sample sizes: control ($n = 9–11$), resilient ($n = 9–11$), and susceptible mice ($n = 19–23$). Error bars represent mean ± SEM. *** indicate $p < 0.001$.

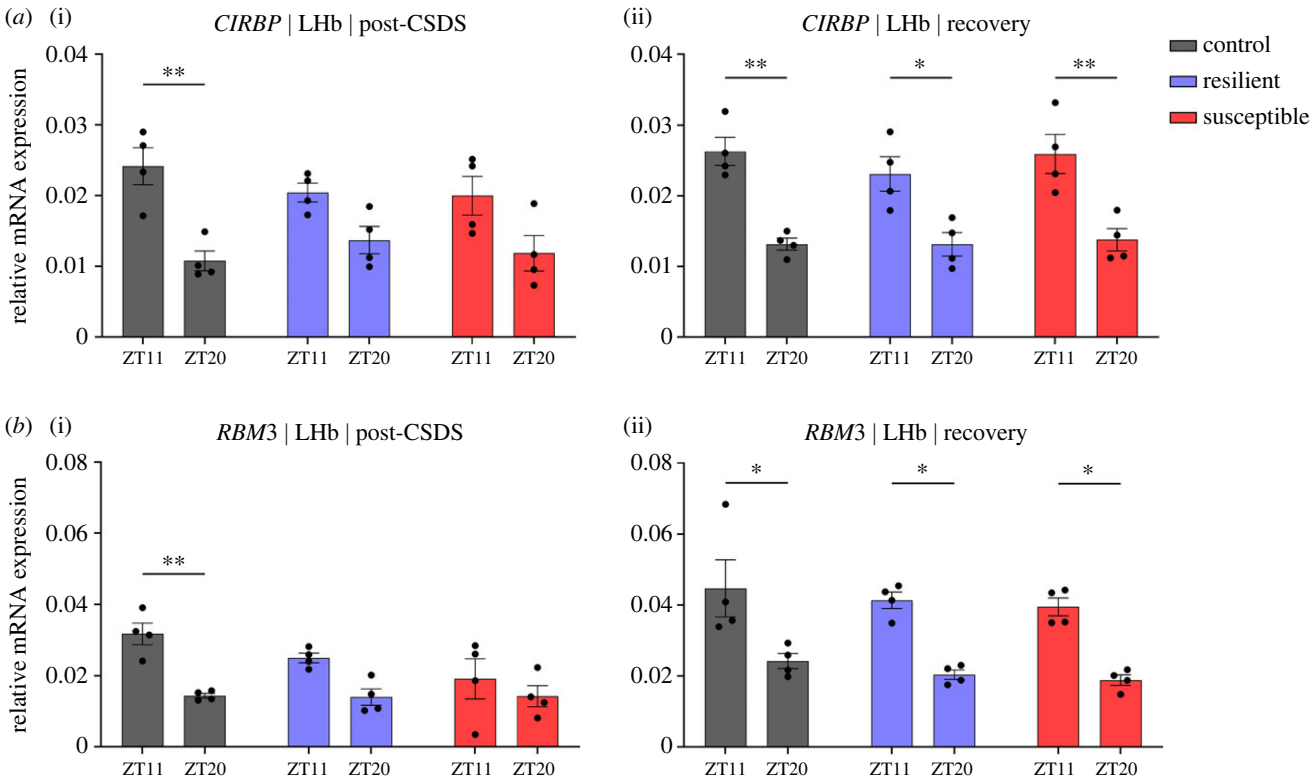

Figure 3. Diurnal rhythmic expression of Cirbp and RBM3 in the LHb is blunted immediately after CSDS. (*a*,*b*)(i) Control, but not resilient and susceptible mice, display significantly larger mRNA expression of Cirbp (Tukey's HSD, $p < 0.01$, 95% C.I. = [0.00, 0.02]) and RBM3 ($p < 0.01$, 95% C.I. = [0.00, 0.03]) in the LHb at ZT11 compared to ZT20 post-CSD. (*a*,*b*)(ii) The molecular rhythms of Cirbp and RBM3 in resilient [Cirbp: $p = 0.02$, 95% C.I. = [0.00, 0.02]; RBM3: $p = 0.01$, 95% C.I. = [0.00, 0.04]] and susceptible [Cirbp: $p < 0.01$, 95% C.I. = [0.00, 0.03]; RBM3: $p = 0.01$, 95% C.I. = [0.00, 0.04]] mice return 10 days after recovery and are at similar levels comparable to control [Cirbp: $p < 0.01$, 95% C.I. = [0.00, 0.02]; RBM3: $p = 0.01$, 95% C.I. = [0.00, 0.04]]. Each experimental group consisted of 4 biological replicates split into 3 technical replicates ($n = 4$). Error bars represent mean ± SEM.* and ** indicate $p < 0.05$ and $p < 0.01$, respectively.

Collection Software and analysed with ClockLab Analysis Software (v. 6.1.10).

2.4. Chronic social defeat stress and behavioural analysis

For a period of 15 days, experimental C57BL6/J mice were exposed daily to an aggressive CD1 resident mouse for 10 min of physical interaction. After each defeat session, C57BL6/J mice were separated from the CD1 mice within the same cage using a perforated Plexiglas divider that allowed for olfactory and visual sensory, but not physical, contact. Daily defeat sessions were consistently carried out between ZT8 and ZT10. C57BL6/J mice were exposed to a novel aggressor each day to avoid familiarization. Control mice were kept in pairs in an equivalent cage set-up, with a Plexiglas divider separating the two control mice at all times. These mice were kept in the same room as experimental mice in order to control for variations in ambient temperature.

To assess social aversion as a measure of depressive-like behaviour, we used the social interaction (SI) test. For each cohort, the SI test was conducted the day following the end of CSDS between ZT6 and ZT10. The test was conducted in a white square Plexiglas arena (dimensions 42 × 42 × 42.5 cm) under red light. The SI test for each mouse consisted of two 2.5 min sessions: one without a CD1 social target and another with an unfamiliar nonaggressive CD1 social target. TopScan was used to track the time each experimental mouse spent in the predefined zones within the arena. Mice were phenotyped based on the social interaction ratio (SI ratio) scores, which was calculated as described previously [32]. Experimental mice with scores < 100 were classified as 'stress-susceptible' and those with scores ≥ 100 were classified as 'stress-resilient'.

2.5. Brain sampling for molecular analysis

Sampling was started 24 h following SI and completed within three days. Mice were anesthetized using 0.25 ml isoflurane (Vedco, St. Joseph, Missouri, USA) and then sacrificed by cervical dislocation followed by decapitation. Extractions were carried out on a cold sterile surface and the extracted brains were directly immersed into cold isopentane (Sigma Aldrich M3263) to be flash-frozen. Brains were sliced on the Leica CM1950 cryostat (Leica Biosystems, Nussloch, Germany), using Mouse Brain Atlas [33] as a reference for identification of the SCN and the LHb. Brain slices were visualized under Leica S Apo Stereozoom 1.0–8.0× stereoscope (Leica Microsystems, Heerburg, Switzerland) and tissue punches of the regions were collected into 1.5 ml DNA LoBind tubes (Eppendorf, Hamburg, Germany). The punches were then snap-frozen using dry ice before being stored at −80°C until RNA isolation.

2.6. RNA isolation and quantitative PCR

RNA was isolated using Qiagen RNeasy Micro Kit, as per manufacturer's instructions, and quantified using Nanodrop 8000 (Thermo Fisher Scientific, Waltham, MA, USA). The isolated RNA was converted to cDNA using the Maxima H Minus First Strand cDNA Synthesis Kit (Thermo Fisher Scientific), as per manufacturer's protocol. The template cDNA was amplified using Qiagen Primers for the transcripts: Hsf1 (NM_008296), Rbm3 (NM_016809), Cirbp (NM_007705) and Prok2 (NM_015768) to quantify levels of mRNA in the SCN and LHb. GAPDH (NM_008804) was used as the reference housekeeping gene in both SCN and LHb, as reported previously [34–39]. Non-template controls were run for each primer pair. qPCR was carried out using Applied Biosystems QuantStudio5 Real-Time PCR System (Thermo Fisher Scientific). All experimental groups for qPCR experiments consisted of four biological replicates split into three technical replicates to ensure accuracy of measurement. The average of the threshold cycle (Ct) was taken across the triplicates and normalized to the GAPDH using the $2^{(\Delta Ct)}$ method. Fold changes were calculated relative to controls using the $2^{(\Delta\Delta Ct)}$ method.

2.7. Statistical analysis

Prism 9 (Graphpad Software, La Jolla, California, USA) was used for data plotting and statistical analyses. Statistical significance was determined using one-way and two-way ANOVAs, two-tailed independent *t*-tests and Tukey's HSD *post hoc* test. All values are expressed as the mean ± standard error of the mean (SEM). The sample size (n) is noted in the specific figure legends for each experiment.

3. Results and discussion

We found that daily rhythms of Tcore are affected by chronic social stress. Prior to stress, all mice exhibited lowest Tcore in the daytime, when mice are least active, and highest at nighttime, where they are most active (figure 2*a*(i,ii)) (electronic supplementary material, table S1). However, during CSDS both resilient and susceptible mice generally exhibited higher Tcore in the daytime and lower Tcore in the nighttime, compared to controls (figure 2*b*(i,ii)). Daytime Tcore of resilient mice returned to control levels immediately after CSDS, while susceptible mice continued to exhibit elevated Tcore for a longer period during the recovery phase (figure 2*c*(i,ii)). During CSDS, both resilient and susceptible mice exhibited significantly lower Tcore amplitudes compared to controls (figure 2*d*) (electronic supplementary material, table S2). However, during the first 5 days of recovery period, Tcore amplitudes were significantly blunted in susceptible, but not resilient mice. By contrast there were no significant differences in Tcore amplitude between control and susceptible from day 6 to day 10 of the recovery period. Furthermore, the interdaily stability (IS) of temperature rhythms during stress was fragmented in all groups which recovered to control levels post stress (figure 2*e*). Our results align with clinical findings that patients with depression exhibit blunted diurnal rhythms where nighttime temperature is abnormally high (when people are usually least active), while daytime temperature is largely unaffected [15]. Preliminary studies in humans suggest that circadian temperature profile predicts stress vulnerability [40–42]. However, since there were no differences at baseline in our study, we failed to model these results using CSDS. Previous studies have shown aberrations in physiological processes in susceptible mice [19,43–45]. It is likely that homeostatic factors that maintain Tcore in resilient mice buffer against stress-induced processes that drive elevated daytime Tcore and greater blunting of Tcore amplitudes in susceptible mice. Our study correlates with previous observations that more severe stress induces significantly greater blunting of temperature rhythms [46]. We had previously shown that susceptible and resilient mice display reduced overall sleep homeostasis [47]. Moreover, susceptible mice exhibited deficient NREM recovery sleep responses and increased NREM sleep fragmentation following CSDS [48,49]. Although affected by locomotion and sleep patterns, Tcore is under tight circadian control which exerts the most powerful influence on its regulation [50]. Since sleep and Tcore are closely related it may be that chronic stress causes pathophysiological changes in circuitry that coregulates sleep architecture and body temperature homeostasis [51,52].

Given the regulatory role of the SCN in governing temperature rhythms, we speculated that additional rhythmic processes influenced by the SCN might also be perturbed by chronic stress. Thus, we recorded locomotor rhythms before and after exposure to CSDS and found these rhythms to be unaffected by chronic stress (electronic supplementary material, figure S3). The three phenotypes exhibited similar bouts of activity, light and dark phase activity profiles, as

well as interdaily and intradaily stability of locomotor rhythms (electronic supplementary material, figure S3). We did not observe any clear correlation pattern between Tcore and locomotor activity in any of the phenotypes or recording phases (electronic supplementary material, figure S8). Since we did not observe any effect of stress on locomotor rhythms, we wondered whether this lack of effect was associated with expression patterns of genes that regulate diurnal cycles of locomotion. Prokineticin 2 (*Prok2*) is one such clock-controlled gene whose product is an important neuropeptide output signal of the SCN that regulates locomotor rhythms [53]. Relatively stable expression of *Prok2* in the SCN of stress-exposed mice, along with rhythmic diurnal locomotor activity, suggests that the SCN is buffered against environmental stressors, enabling normal light entrainment (electronic supplementary material, figure S4*a*(i,ii)). In line with this hypothesis, we observed similar *BMAL1* expression patterns in the SCN across the three phenotypes (electronic supplementary material, figure S4*b*(i,ii)). Relatedly, clock gene expression following chronic mild stress (CMS) was shown to be stable in the SCN but not in the other regions involved in mood regulation [54]. Previous light pulse experiments on stress-exposed and control mice revealed phase delay of the body temperature rhythm without any changes in the circadian pacemaker functions [55]. Our findings on locomotor activity and *Prok2* expression match previous studies and indicate that pacemaker function remains unaffected by different forms of chronic stress (electronic supplementary material, figures S3 and S4) [54,55].

Next, we investigated whether expression of the thermosensitive genes *Rbm3*, *Cirbp* and *Hsf1* correlates with the observed changes in temperature profiles immediately after CSDS and 10 days of recovery. *Rbm3* and *Cirbp* are both expressed in response to lower temperatures, with their baseline expression oscillating diurnally and being linked to circadian function [7,56,57]. The expression of *Rbm3* and *Cirbp* in the LHb of control mice was significantly higher in the day (ZT11), when Tcore is lower, compared to the night (ZT20), when Tcore is higher (figure 3*a*(i),*b*(i)). By contrast, immediately after CSDS, there was no significant difference in daytime and night-time expression of *Rbm3* and *Cirbp* in the LHb of susceptible and resilient mice. However, after 10 days of recovery, the diurnal differences in expression of *Rbm3* and *Cirbp* in the LHb of both susceptible and resilient mice were similar to control mice (figure 3*a*(ii),*b*(ii)), suggesting recovery of daily rhythmic expression following the recovery of temperature rhythms. *Hsf1* did not show robust rhythms in the LHb (electronic supplementary material, figure S5). Studies have shown that exposure to decreased temperature (cold shock) does not generate a significant expression of *Hsf1*, consistent with the findings from our study [58]. Additionally, the lack of significant changes within the LHb suggest possible region-specific differences in rhythmic expression following exposure to chronic stress (electronic supplementary material, figure S5).

These results are supported by previous findings that mild hypothermia results in peak expression of *Cirbp* and *Rbm3* which decreases significantly following deep hypothermia [12]. In turn, hyperthermia causes substantial decreases in expression of both of these genes in cultured mammalian cells [12]. CMS affects rhythmic expression of clock genes in various brain regions, including the LHb [54]. We suggest that chronic stress disrupts Tcore resulting in perturbations of thermosensitive gene expression which then impacts clock gene expression in the long-term. This eventually results in pathophysiological changes in the LHb [21]. Since we did not see any stress induced changes in clock-controlled gene expression we do not think stress directly disrupts thermosensitive gene expression. To the best of our knowledge, the selected thermosensitive genes do not affect temperature regulation directly. Additionally, the identical pattern of blunting observed in core body temperature and expression of these genes in the LHb at the same time points further suggests that it is core body temperature that causes this gene expression blunting rather than an independent CSDS-induced mechanism. Further experiments involving higher temporal resolution and examination of additional clock genes are necessary, to support our conclusion. Further experiments involving higher temporal resolution and examination of additional clock genes are necessary, to support our conclusion. Our observations on the effect of stress on temperature and molecular rhythms are in close agreement with previous findings where repeated 5-day social defeat stress resulted in decreased amplitude of heart rate and body temperature persisting for at least 10-days after the final confrontation [59]. *Rbm3* regulates local synaptic translation and neuronal activity, and knockdown of *Rbm3* at specific times of the day increases firing of cultured hippocampal cells [57]. Increased expression of *Cirbp* when mice are asleep, possibly because of lower Tcore associated with lower motor activity, attenuates expression of wake-inducing/sustaining genes, such as *Homer*. By contrast, sleep deprivation leads to increased expression of wake-inducing genes because of prolonged attenuation of *Cirbp* expression, possibly because of elevated Tcore as a result of greater activity [60]. We speculate that such evidence points to the mechanism by which stress induces fragmented sleep resulting in decreased *Cirb* expression and, consequently, greater expression of wake-promoting genes that cause further sleep fragmentation. Future studies are warranted to investigate this putative feedforward mechanism and its role in interlinking mood disorders, fragmented sleep and Tcore changes.

4. Conclusion

Taken together, this study provides additional evidence for stress-induced changes in temperature regulation and differential expression of thermo-sensitive genes. Importantly, we identified physiological differences in daily temperature profiles between susceptible and resilient mice. As such, this study represents a crucial step towards a more systematic understanding of the temperature imbalances experienced by patients diagnosed with mood disorders. The preliminary findings of this study highlight the interplay between temperature dysregulation and thermosensitive gene expression in the LHb. One limitation of this study is the lack of multiple sampling timepoints across the day/night cycle that would better assess rhythmic gene expression with higher resolution. Future studies are warranted to include more timepoints and investigate rhythmicity of expression of other clock genes in response to stress. Some genes may appear relatively unaffected at the mRNA levels but their protein levels may be altered. Future experiments to investigate the changes in protein expression would enable an additional level of insight into the effects of stress on core body temperature regulation. Moreover, investigation to determine if there are instances where changes in Tcore increase stress vulnerability are also

warranted. Overall, such studies would help clarify the cause and consequence in the interplay between core temperature and clock-modulating thermosensitive genes.

Ethics. Animal protocols have been approved by the National Institute of Health Guide for Care and Use of Laboratory Animals (IACUC Protocol: 150005A2, 19-0004A1), as well as the NYUAD Animal Care and Use Committee.

Data accessibility. All relevant data are within the paper and its files.

Additional information is provided in electronic supplementary material [61].

Authors' contributions. S.H.: conceptualization, data curation, formal analysis, investigation; P.N.: conceptualization, data curation, formal analysis, investigation, methodology, project administration, supervision, writing—original draft, writing—review and editing; M.A.H.: conceptualization, data curation, formal analysis, investigation, methodology; A.P.: formal analysis, methodology, writing—review and editing; M.S.: data curation, methodology; V.M.: conceptualization, data curation, investigation, methodology; D.C.: conceptualization, formal analysis, funding acquisition, project administration, resources, supervision, writing—original draft, writing—review and editing.

All authors gave final approval for publication and agreed to be held accountable for the work performed therein.

Conflict of interest declaration. We declare we have no competing interests.

Funding. The funders had no role in study design, data collection and analysis, decision to publish, or preparation of the manuscript.

References

1. Buhr ED, Yoo S-H, Takahashi JS. 2010 Temperature as a universal resetting cue for mammalian circadian oscillators. *Science* **330**, 379–385. (doi:10.1126/science.1195262)
2. Xie Y, Tang Q, Chen G, Xie M, Yu S, Zhao J, Chen L. 2019 New insights into the circadian rhythm and its related diseases. *Front. Physiol.* **10**, 682. (doi:10.3389/fphys.2019.00682)
3. Morrison SF, Madden CJ. 2014 Central nervous system regulation of brown adipose tissue. In *Comprehensive physiology* (ed. R Terjung), pp. 1677–1713. Chichester, UK: Wiley.
4. Morrison SF, Nakamura K. 2019 Central mechanisms for thermoregulation. *Annu. Rev. Physiol.* **81**, 285–308. (doi:10.1146/annurev-physiol-020518-114546)
5. Weinert D. 2010 Circadian temperature variation and ageing. *Ageing Research Reviews* **9**, 51–60. (doi:10.1016/j.arr.2009.07.003)
6. Morf J, Schibler U. 2013 Body temperature cycles: gatekeepers of circadian clocks. *Cell Cycle* **12**, 539–540. (doi:10.4161/cc.23670)
7. Coiffard B, Diallo AB, Mezouar S, Leone M, Mege J-L. 2021 A tangled threesome: circadian rhythm, body temperature variations, and the immune system. *Biology* **10**, 65. (doi:10.3390/biology10010065)
8. Nam D, Yechoor VK, Ma K. 2016 Molecular clock integration of brown adipose tissue formation and function. *Adipocyte* **5**, 243–250. (doi:10.1080/21623945.2015.1082015)
9. Saini C, Morf J, Stratmann M, Gos P, Schibler U. 2012 Simulated body temperature rhythms reveal the phase-shifting behavior and plasticity of mammalian circadian oscillators. *Genes Dev.* **26**, 567–580. (doi:10.1101/gad.183251.111)
10. Liu Y, Hu W, Murakawa Y, Yin J, Wang G, Landthaler M, Yan J. 2013 Cold-induced RNA-binding proteins regulate circadian gene expression by controlling alternative polyadenylation. *Sci. Rep.* **3**, 2054. (doi:10.1038/srep02054)
11. Schibler U *et al.* 2015 Clock-talk: interactions between central and peripheral circadian oscillators in mammals. *Cold Spring Harb. Symp. Quant. Biol.* **80**, 223–232. (doi:10.1101/sqb.2015.80.027490)
12. Zhu X, Bührer C, Wellmann S. 2016 Cold-inducible proteins CIRP and RBM3, a unique couple with activities far beyond the cold. *Cell Mol. Life Sci.* **73**, 3839–3859. (doi:10.1007/s00018-016-2253-7)
13. Zhong P, Huang H. 2017 Recent progress in the research of cold-inducible RNA-binding protein. *Future Sci. OA* **3**, FSO246. (doi:10.4155/fsoa-2017-0077)
14. Karatsoreos IN. 2012 Effects of circadian disruption on mental and physical health. *Curr. Neurol. Neurosci. Rep.* **12**, 218–225. (doi:10.1007/s11910-012-0252-0)
15. Bunney BG *et al.* 2015 Circadian dysregulation of clock genes: clues to rapid treatments in major depressive disorder. *Mol. Psychiatry* **20**, 48–55. (doi:10.1038/mp.2014.138)
16. Edgar N, McClung CA. 2013 Major depressive disorder: a loss of circadian synchrony? *Bioessays* **35**, 940–944. (doi:10.1002/bies.201300086)
17. Ootsuka Y, Mohammed M. 2015 Activation of the habenula complex evokes autonomic physiological responses similar to those associated with emotional stress. *Physiol. Rep.* **3**, e12297. (doi:10.14814/phy2.12297)
18. Brizuela M, Antipov A, Blessing WW, Ootsuka Y. 2019 Activating dopamine D2 receptors reduces brown adipose tissue thermogenesis induced by psychological stress and by activation of the lateral habenula. *Sci. Rep.* **9**, 19512. (doi:10.1038/s41598-019-56125-3)
19. Chaudhury D *et al.* 2013 Rapid regulation of depression-related behaviours by control of midbrain dopamine neurons. *Nature* **493**, 532–536. (doi:10.1038/nature11713)
20. Yang Y, Cui Y, Sang K, Dong Y, Ni Z, Ma S, Hu H. 2018 Ketamine blocks bursting in the lateral habenula to rapidly relieve depression. *Nature* **554**, 317–322. (doi:10.1038/nature25509)
21. Liu H *et al.* 2021 Blunted diurnal firing in lateral habenula projections to dorsal raphe nucleus and delayed photoentrainment in stress-susceptible mice. *PLoS Biol.* **19**, e3000709. (doi:10.1371/journal.pbio.3000709)
22. Zheng Z *et al.* 2022 Hypothalamus-habenula potentiation encodes chronic stress experience and drives depression onset. *Neuron* **110**, 1400–1415. (doi:10.1016/j.neuron.2022.01.011)
23. Mendoza J, Vanotti G. 2019 Circadian neurogenetics of mood disorders. *Cell Tissue Res.* **377**, 81–94. (doi:10.1007/s00441-019-03033-7)
24. Barna J, Csermely P, Vellai T. 2018 Roles of heat shock factor 1 beyond the heat shock response. *Cell. Mol. Life Sci.* **75**, 2897–2916. (doi:10.1007/s00018-018-2836-6)
25. Costa M *et al.* 2015 Preliminary transcriptome analysis in lymphoblasts from cluster headache and bipolar disorder patients implicates dysregulation of circadian and serotonergic genes. *J. Mol. Neurosci.* **56**, 688–695. (doi:10.1007/s12031-015-0567-9)
26. Kawamura G, Hattori M, Takamatsu K, Tsukada T, Ninomiya Y, Benjamin I, Sassone-Corsi P, Ozawa T, Tamaru T. 2018 Cooperative interaction among BMAL1, HSF1, and p53 protects mammalian cells from UV stress. *Commun. Biol.* **1**, 204. (doi:10.1038/s42003-018-0209-1)
27. Uchida S *et al.* 2011 Impaired hippocampal spinogenesis and neurogenesis and altered affective behavior in mice lacking heat shock factor 1. *Proc. Natl Acad. Sci. USA* **108**, 1681–1686. (doi:10.1073/pnas.1016424108)
28. Chapon P-A, Bulla J, Besnard S, Gauthier A, Bessot N. 2018 Performances assessment of Anipill ® device prototype designed for continuous temperature monitoring. *Biomed. Phys. Eng. Express* **4**, 055020. (doi:10.1088/2057-1976/aad440)
29. Moore A, Zielinski T, Millar AJ. 2014 Online period estimation and determination of rhythmicity in circadian data, using the BioDare data infrastructure. In *Plant circadian networks* (ed. D Staiger), pp. 13–44. New York, NY: Springer.
30. Blume C, Santhi N, Schabus M. 2016 'nparACT' package for R: A free software tool for the non-parametric analysis of actigraphy data. *MethodsX* **3**, 430–435. (doi:10.1016/j.mex.2016.05.006)
31. Cavalcanti-Ferreira P, Berk L, Daher N, Campus T, Araujo J, Petrofsky J, Lohman E. 2018 A nonparametric methodological analysis of rest-activity rhythm in type 2 diabetes. *Sleep Sci.* **11**, 281–289. (doi:10.5935/1984-0063.20180044)
32. Golden SA, Covington HE, Berton O, Russo SJ. 2011 A standardized protocol for repeated social defeat

stress in mice. *Nat. Protoc.* **6**, 1183–1191. (doi:10.1038/nprot.2011.361)

33. Paxinos G, Franklin KBJ. 2019 *Paxinos and franklin's The mouse brain in stereotaxic coordinates*, 5th edn. London: Academic Press.
34. Pembroke WG, Babbs A, Davies KE, Ponting CP, Oliver PL. 2015 Temporal transcriptomics suggest that twin-peaking genes reset the clock. *Elife* **4**, e10518. (doi:10.7554/eLife.10518)
35. Meng Q-J *et al.* 2008 Setting clock speed in mammals: the CK1 epsilon tau mutation in mice accelerates circadian pacemakers by selectively destabilizing PERIOD proteins. *Neuron* **58**, 78–88. (doi:10.1016/j.neuron.2008.01.019)
36. Park H, Rhee J, Lee S, Chung C. 2017 Selectively impaired endocannabinoid-dependent long-term depression in the lateral habenula in an animal model of depression. *Cell Rep.* **20**, 289–296. (doi:10.1016/j.celrep.2017.06.049)
37. Yang N *et al.* 2020 Quantitative live imaging of Venus::BMAL1 in a mouse model reveals complex dynamics of the master circadian clock regulator. *PLoS Genet.* **16**, e1008729. (doi:10.1371/journal.pgen.1008729)
38. Gerstner JR, Vander Heyden WM, Lavaute TM, Landry CF. 2006 Profiles of novel diurnally regulated genes in mouse hypothalamus: expression analysis of the cysteine and histidine-rich domain-containing, zinc-binding protein 1, the fatty acid-binding protein 7 and the GTPase, ras-like family member 11b. *Neuroscience* **139**, 1435–1448. (doi:10.1016/j.neuroscience.2006.01.020)
39. Poller WC, Bernard R, Derst C, Weiss T, Madai VI, Veh RW. 2011 Lateral habenular neurons projecting to reward-processing monoaminergic nuclei express hyperpolarization-activated cyclic nucleotid-gated cation channels. *Neuroscience* **193**, 205–216. (doi:10.1016/j.neuroscience.2011.07.013)
40. Magal N, Rab SL, Goldstein P, Simon L, Jiryis T, Admon R. 2022 Predicting chronic stress among healthy females using daily-life physiological and lifestyle features from wearable sensors. *Chronic Stress* **6**, 247054702211009. (doi:10.1177/24705470221100987)
41. Taylor S, Jaques N, Nosakhare E, Sano A, Picard R. 2020 Personalized multitask learning for predicting tomorrow's mood, stress, and health. *IEEE Trans. Affective Comput.* **11**, 200–213. (doi:10.1109/TAFFC.2017.2784832)
42. Sano A, Taylor S, McHill AW, Phillips AJ, Barger LK, Klerman E, Picard R. 2018 Identifying objective physiological markers and modifiable behaviors for self-reported stress and mental health status using wearable sensors and mobile phones: observational study. *J. Med. Internet Res.* **20**, e210. (doi:10.2196/jmir.9410)
43. Krishnan V *et al.* 2007 Molecular adaptations underlying susceptibility and resistance to social defeat in brain reward regions. *Cell* **131**, 391–404. (doi:10.1016/j.cell.2007.09.018)
44. Friedman AK *et al.* 2014 Enhancing depression mechanisms in midbrain dopamine neurons achieves homeostatic resilience. *Science* **344**, 313–319. (doi:10.1126/science.1249240)
45. Chaudhury D, Liu H, Han M-H. 2015 Neuronal correlates of depression. *Cell. Mol. Life Sci.* **72**, 4825–4848. (doi:10.1007/s00018-015-2044-6)
46. Kant GJ, Bauman RA, Pastel RH, Myatt CA, Closser-Gomez E, D'Angelo CP. 1991 Effects of controllable vs. uncontrollable stress on circadian temperature rhythms. *Physiol. Behav.* **49**, 625–630. (doi:10.1016/0031-9384(91)90289-Z)
47. Radwan B, Yanez Touzet A, Hammami S, Chaudhury D. 2021 Prolonged exposure to social stress impairs homeostatic sleep regulation. *Front. Neurosci.* **15**, 633955. (doi:10.3389/fnins.2021.633955)
48. Radwan B, Jansen G, Chaudhury D. 2021 Abnormal sleep signals vulnerability to chronic social defeat stress. *Front. Neurosci.* **14**, 610655. (doi:10.3389/fnins.2020.610655)
49. Radwan B, Jansen G, Chaudhury D. 2021 Sleep-wake dynamics pre- and post-exposure to chronic social stress. *iScience* **24**, 103204. (doi:10.1016/j.isci.2021.103204)
50. Refinetti R. 2020 Circadian rhythmicity of body temperature and metabolism. *Temperature (Austin)* **7**, 321–362. (doi:10.1080/23328940.2020.1743605)
51. Harding EC, Franks NP, Wisden W. 2020 Sleep and thermoregulation. *Curr. Opin. Physiol.* **15**, 7–13. (doi:10.1016/j.cophys.2019.11.008)
52. Harding EC *et al.* 2018 A neuronal hub binding sleep initiation and body cooling in response to a warm external stimulus. *Curr. Biol.* **28**, 2263–2273.e4. (doi:10.1016/j.cub.2018.05.054)
53. Li J-D, Hu W-P, Boehmer L, Cheng MY, Lee AG, Jilek A, Siegel JM, Zhou Q-Y. 2006 Attenuated circadian rhythms in mice lacking the *Prokineticin 2* Gene. *J. Neurosci.* **26**, 11 615–11 623. (doi:10.1523/JNEUROSCI.3679-06.2006)
54. Christiansen S, Bouzinova E, Fahrenkrug J, Wiborg O. 2016 Altered expression pattern of clock genes in a rat model of depression. *IJNPPY* **19**, pyw061. (doi:10.1093/ijnp/pyw061)
55. Meerlo P, Van Den Hoofdakker RH, Koolhaas JM, Daan S. 1997 Stress-induced changes in circadian rhythms of body temperature and activity in rats are not caused by pacemaker changes. *J. Biol. Rhythms* **12**, 80–92. (doi:10.1177/074873049701200109)
56. Nishiyama H, Xue J-H, Sato T, Fukuyama H, Mizuno N, Houtani T, Sugimoto T, Fujita J. 1998 Diurnal change of the cold-inducible RNA-binding protein (Cirp) expression in mouse brain. *Biochem. Biophys. Res. Commun.* **245**, 534–538. (doi:10.1006/bbrc.1998.8482)
57. Sertel SM, Von Elling-Tammen MS, Rizzoli SO. 2021 The mRNA-Binding Protein RBM3 Regulates Activity Patterns and Local Synaptic Translation in Cultured Hippocampal Neurons. *J. Neurosci.* **41**, 1157–1173. (doi:10.1523/JNEUROSCI.0921-20.2020)
58. Roobol A, Carden MJ, Newsam RJ, Smales CM. 2009 Biochemical insights into the mechanisms central to the response of mammalian cells to cold stress and subsequent rewarming: The cold stress response in mammalian cells. *FEBS Journal* **276**, 286–302. (doi:10.1111/j.1742-4658.2008.06781.x)
59. Tornatzky W, Miczek KA. 1993 Long-term impairment of autonomic circadian rhythms after brief intermittent social stress. *Physiol. Behav.* **53**, 983–993. (doi:10.1016/0031-9384(93)90278-N)
60. Hoekstra MM, Emmenegger Y, Hubbard J, Franken P. 2019 Cold-inducible RNA-binding protein (CIRBP) adjusts clock-gene expression and REM-sleep recovery following sleep deprivation. *Elife* **8**, e43400. (doi:10.7554/eLife.43400)
61. Haniffa S, Narain P, Hughes MA, Petković A, Šušić M, Mlambo V, Chaudhury D. 2023 Chronic social stress blunts core body temperature and molecular rhythms of *Rbm3* and *Cirbp* in mouse lateral habenula. Figshare. (doi:10.6084/m9.figshare.c.6730010)